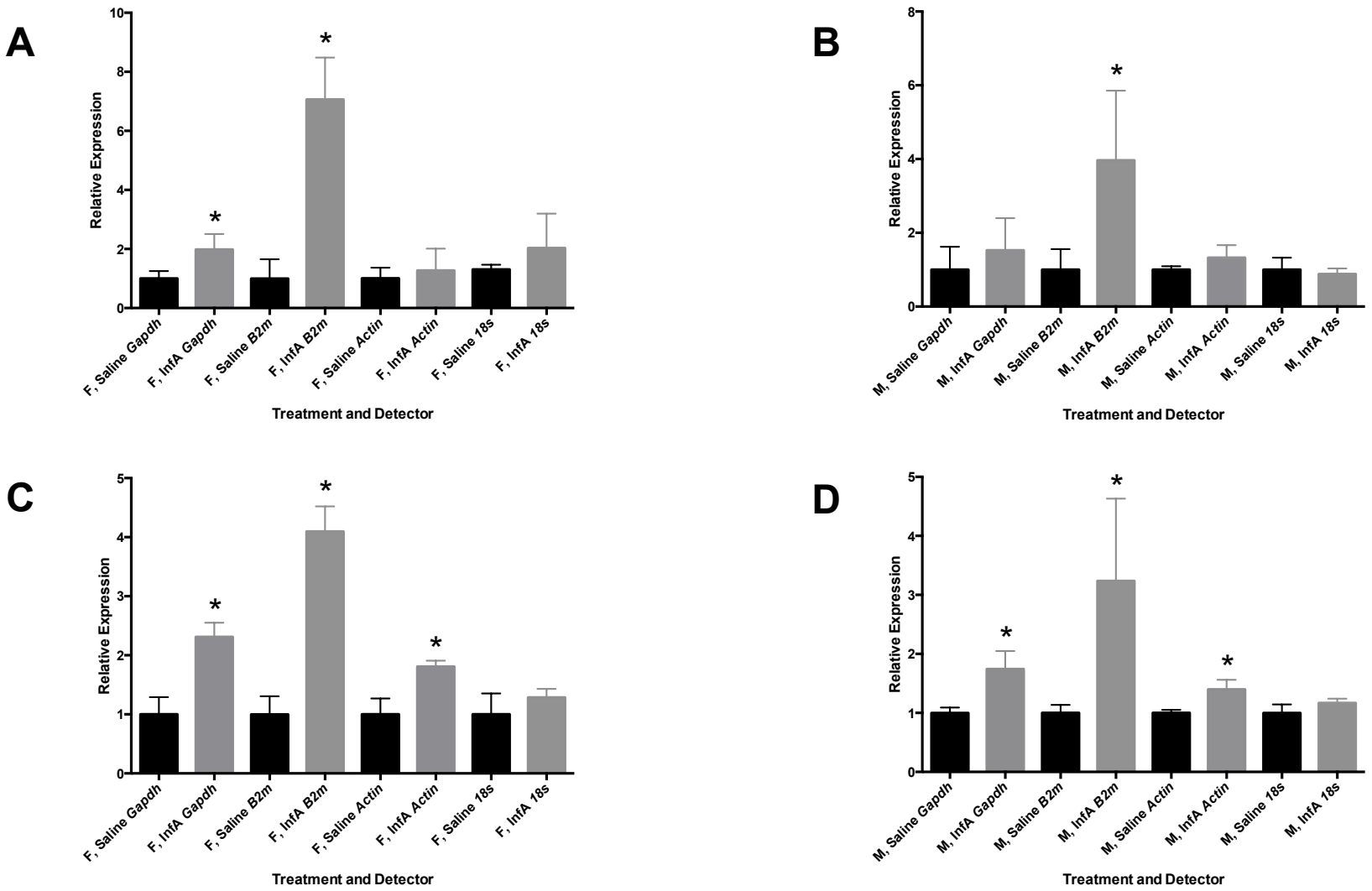

Supplemental Figure 1. Comparison of the relative expression of *Gapdh*, *B2m*, *Actin* and *18s* housekeeping genes in lungs from mice treated with Influenza A or saline. The TaqMan® primer/probes (A) and SYBR® Green primer sets (C) show that expression of *Gapdh, B2m* and *Actin* is increased in female mice after Influenza A treatment. Similar results were obtained for male mice using TaqMan® primer/probes (B) and SYBR® Green primer sets (D). Data shown are mean ± SE; n=6 per group; *p < 0.05 vs. saline control.

Quantitative Polymerase Chain Reaction Analysis of the Mouse *Cyp2j* Subfamily: Tissue Distribution and Regulation
Joan P. Graves, Artiom Gruzdev, J. Alyce Bradbury, Laura M. DeGraff, Huiling Li, John S. House, Samantha L. Hoopes, Matthew L. Edin, and Darryl C. Zeldin
Drug Metabolism and Disposition

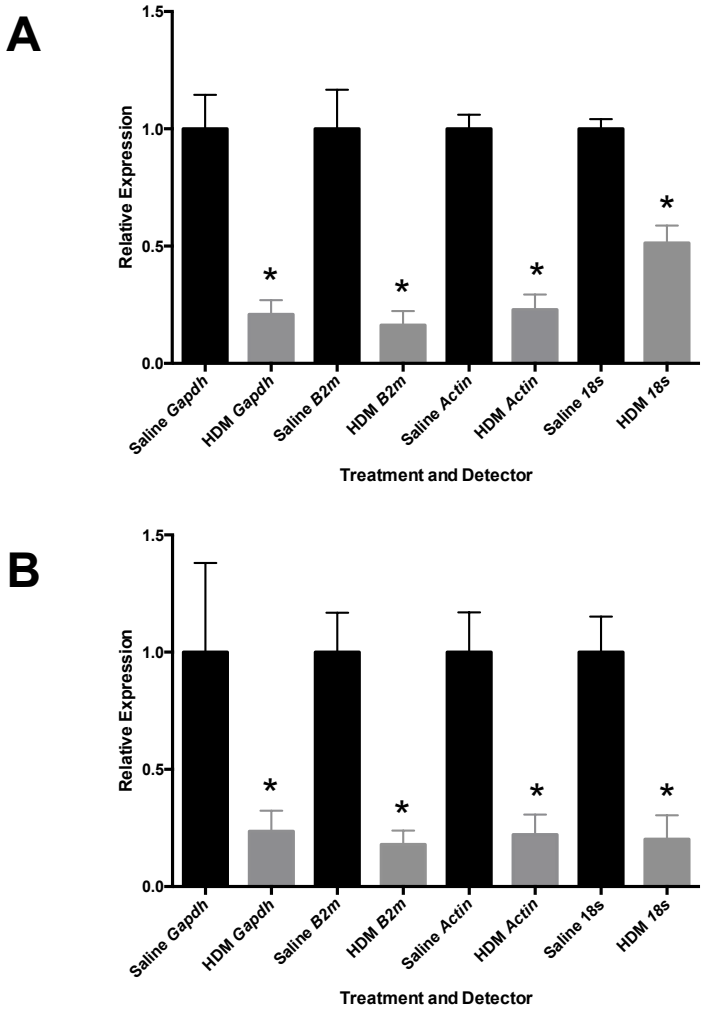

Supplemental Figure 2. Relative expression of *Gapdh*, *B2m*, *Actin* and *18s* housekeeping genes in lungs of mice treated with HDM or saline. The TaqMan® primer/probes (A) and SYBR® Green primer sets (B) showed a significant decrease in expression *Gapdh, B2m, Actin* and *18S* in the HDM-treated lungs. Data shown are mean ± SE; n=6 per group; *p < 0.05 vs. saline control.

Quantitative Polymerase Chain Reaction Analysis of the Mouse *Cyp2j* Subfamily: Tissue Distribution and Regulation
Joan P. Graves, Artiom Gruzdev, J. Alyce Bradbury, Laura M. DeGraff, Huiling Li, John S. House, Samantha L. Hoopes, Matthew L. Edin, and Darryl C. Zeldin
Drug Metabolism and Disposition

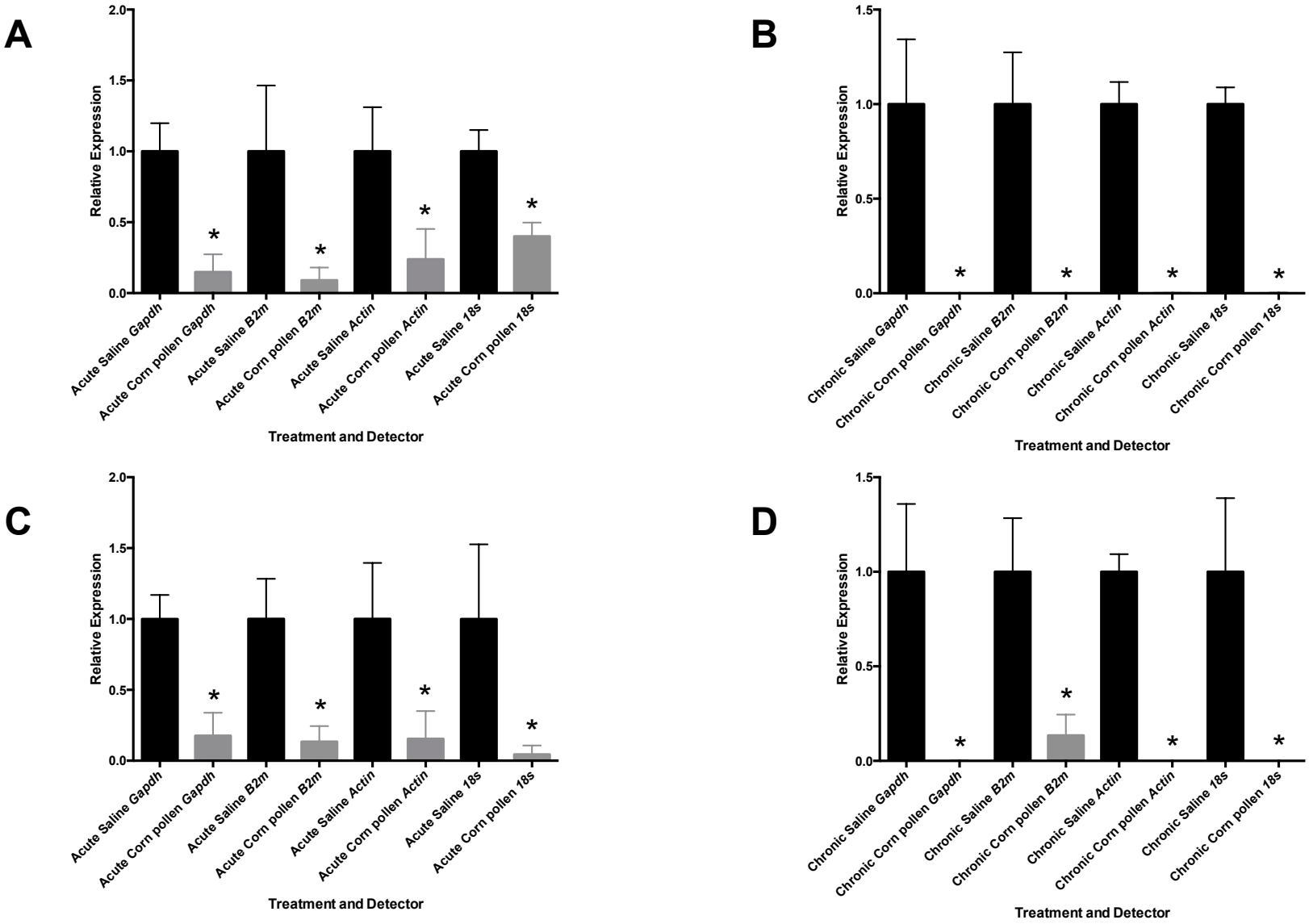

Supplemental Figure 3. Relative expression of *Gapdh*, *B2m*, *Actin* and *18s* housekeeping genes in lungs from mice treated with corn pollen or saline. The TaqMan® primer/probes in acute (A) and chronic (B) exposure models show a significant decrease in expression of the four housekeeping genes in mice exposed to corn pollen. Similar results were obtained with the SYBR® Green primer sets for acute (C) and chronic (D) exposure to corn pollen. Data shown are mean ± SE; n=6 per group; *p < 0.05 vs. saline control.

Quantitative Polymerase Chain Reaction Analysis of the Mouse *Cyp2j* Subfamily: Tissue Distribution and Regulation
Joan P. Graves, Artiom Gruzdev, J. Alyce Bradbury, Laura M. DeGraff, Huiling Li, John S. House, Samantha L. Hoopes, Matthew L. Edin, and Darryl C. Zeldin
Drug Metabolism and Disposition

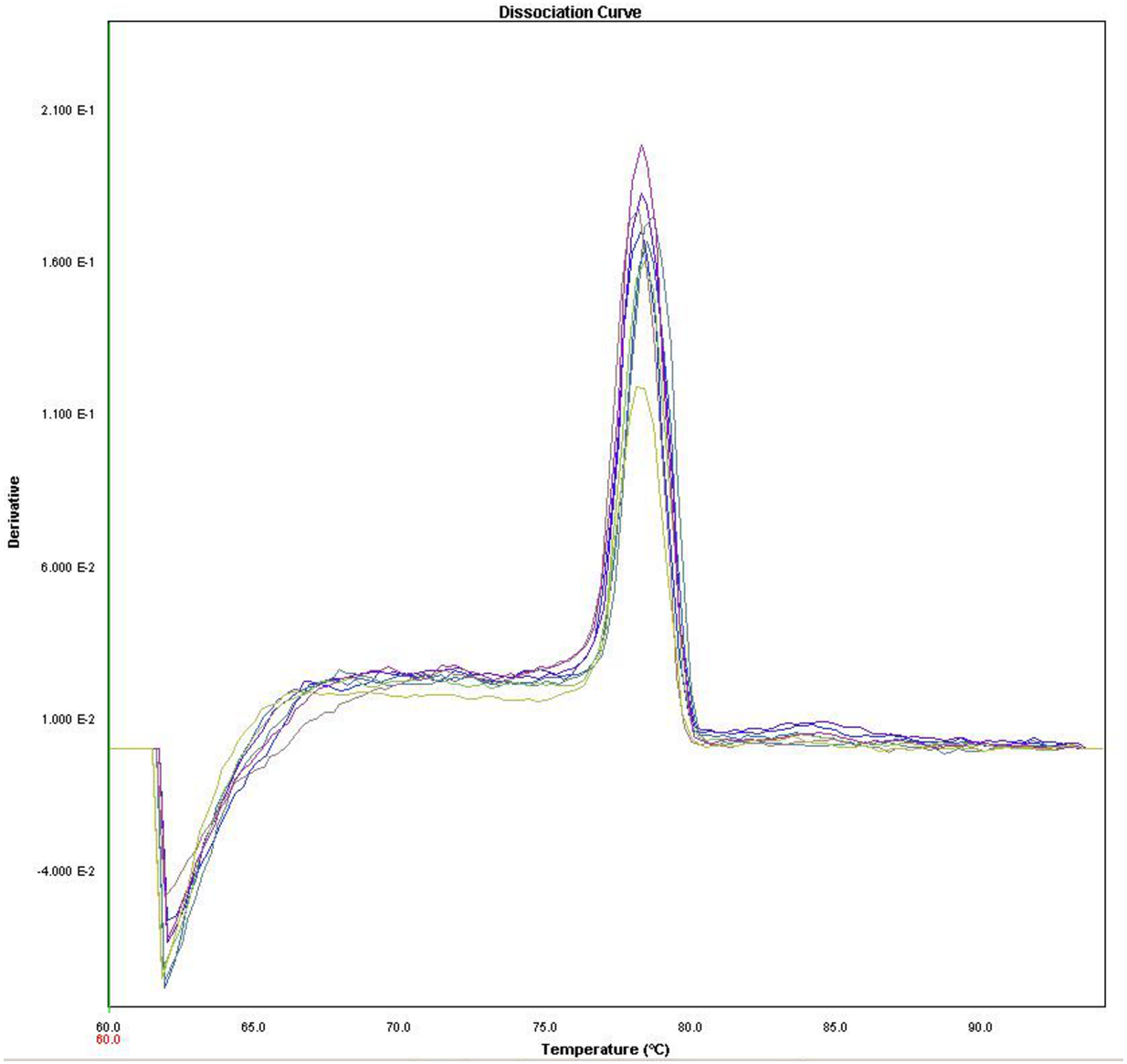

Supplemental Figure 4. Representative dissociation curves of *Cyp2j8* SYBR® Green primer set for brain, lung, liver, fat, ovary and small intestine. Single peaks highly suggest that amplicons in all six tissues are *Cyp2j8*-derived.

Quantitative Polymerase Chain Reaction Analysis of the Mouse *Cyp2j* Subfamily: Tissue Distribution and Regulation
Joan P. Graves, Artiom Gruzdev, J. Alyce Bradbury, Laura M. DeGraff, Huiling Li, John S. House, Samantha L. Hoopes, Matthew L. Edin, and Darryl C. Zeldin
Drug Metabolism and Disposition

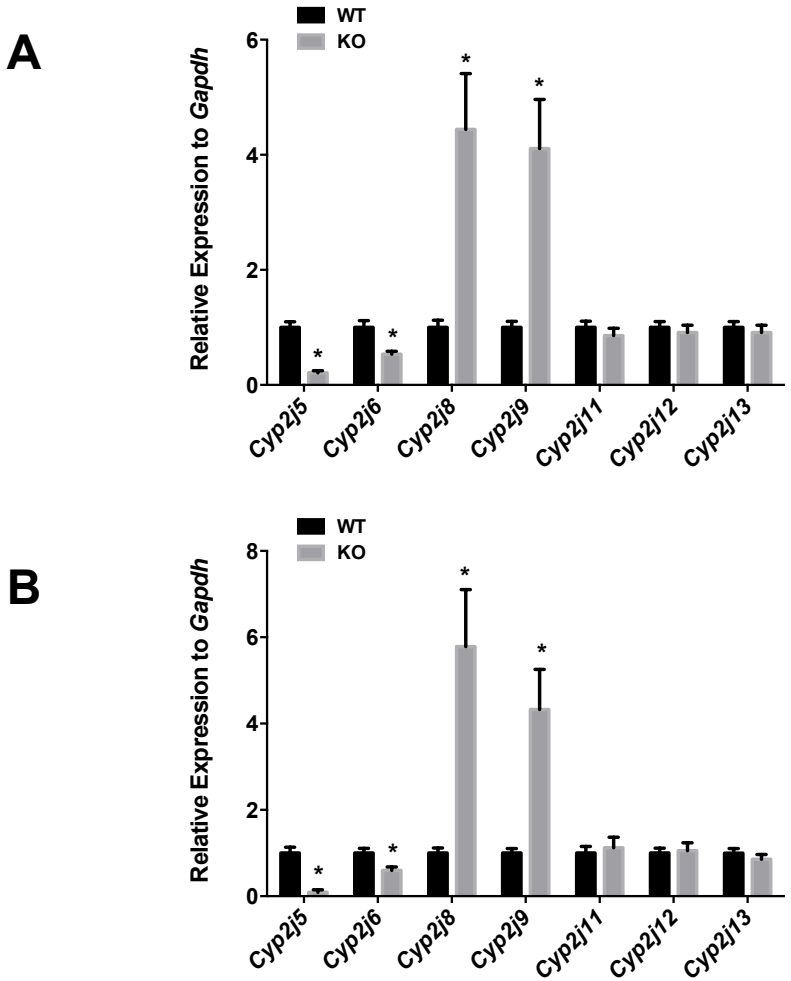

Supplemental Figure 5. Detection of the mouse *Cyp2j* isoforms in *Cyp2j5* WT and KO liver. Both the *Cyp2j5* TaqMan® primer/probe (A) and the SYBR® Green primer set (B) revealed significantly lower *Cyp2j5* expression in the KO liver. As seen in the kidney, *Cyp2j8 and Cyp2j9* were increased in the *Cyp2j5* KO liver relative to WT liver for both the TaqMan® primer/probe (A) and the SYBR® Green primer sets (B). However, *Cyp2j6* expression was decreased in the *Cyp2j5* KO liver relative to WT liver using both the TaqMan® primer probe (A) and the SYBR® Green primer sets (B). This is in contrast to the increase of *Cyp2j6* expression in *Cyp2j5* KO kidney relative to WT kidney for both sets of qPCR (Figure 8). Data shown are mean ± SE, n = 6 per group, *p< 0.05 vs WT.

Quantitative Polymerase Chain Reaction Analysis of the Mouse *Cyp2j* Subfamily: Tissue Distribution and Regulation
Joan P. Graves, Artiom Gruzdev, J. Alyce Bradbury, Laura M> DeGraff, Huiling Li, John S. House, Samantha L. Hoopes, Matthew L. Edin, and Darryl C. Zeldin
Drug Metabolism and Disposition

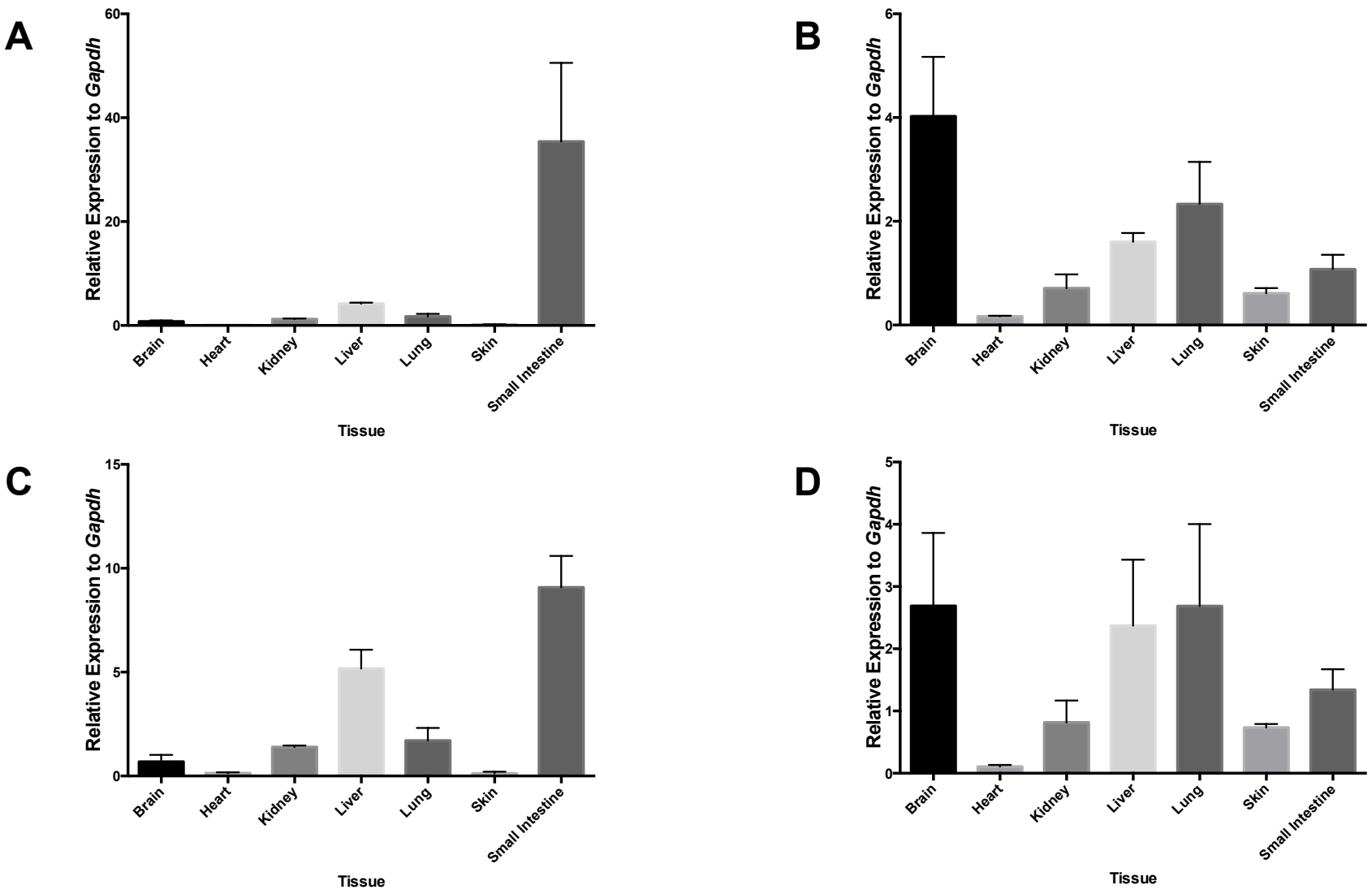

Supplemental Figure 6. Tissue distribution of mouse *Cyp2j6* and *Cyp2j9* in male BALB/C mice. The expression profiles of *Cyp2j6* and *Cyp2j9* in BALB/C mice are examples of the similar profiles to the expression profiles in C57BL/6 mice. As in C57BL/6 mice (Fig. 2), BALB/C mice have the highest expression for *Cyp2j6* in small intestine for both the TaqMan® primer/probe (A) and SYBR® Green primer set (C). As in C57BL/6 mice (Fig. 4), BALB/C mice have the highest expression for *Cyp2j9* in brain, lung, and liver for both the TaqMan® primer/probe (B) and SYBR® Green primer set (D). Data shown are mean ± SE, n= 3 per group.

Quantitative Polymerase Chain Reaction Analysis of the Mouse *Cyp2j* Subfamily: Tissue Distribution and regulation
Joan P. Graves, Artiom Gruzdev, J. Alyce Bradbury, Laura M. DeGraff, Huiling Li, John S. House, Samantha L. Hoopes, Matthew L. Edin, and Darryl C. Zeldin
Drug Metabolism and Disposition

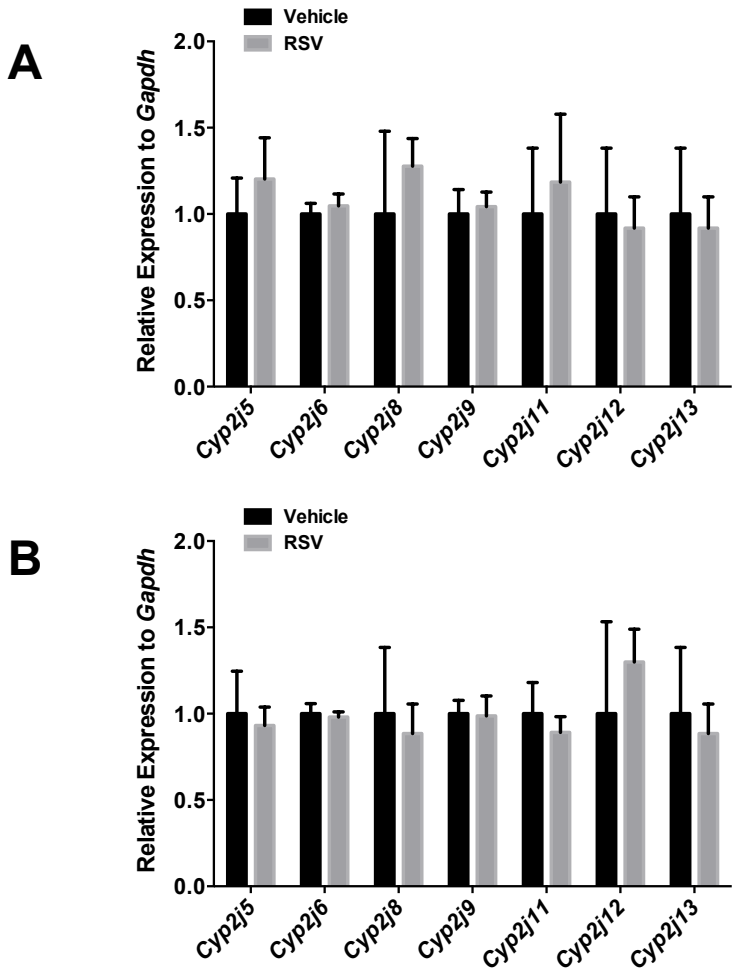

Supplemental Figure 7. Detection of the mouse *Cyp2j* isoforms in lungs of mice treated with human respiratory syncytial virus (RSV) or vehicle. Male C57BL/6 mice were infected with $1x10^7$ PFU/ml of the RSV strain RSV19 or Hep2 cell lysate as a control in a 50µl volume by intranasal instillation. Lungs were collected 5 days after infection. None of the mouse *Cyp2j* isoforms were significantly reduced or increased in the RSV treated mice when compared to vehicle controls using both TaqMan® primer/probes (A) and SYBR® Green primer sets (B). Data shown are mean ± SE, n=3 per group.

Quantitative Polymerase Chani Reaction Analysis of the Mouse *Cyp2j* Subfamily: Tissue Distribution and Regulation
Joan P. Graves, Artiom Gruzdev, J. Alyce Bradbury, Laura M. DeGraff, Huiling Li, John S. House, Samnatha L. Hoopes, Matthew L. Edin, and Darryl C. Zeldin
Drug Metabolism and Disposition